

Review

Quantum simulation of quantum many-body systems with ultracold two-electron atoms in an optical lattice

By Yoshiro TAKAHASHI*^{1,†}

(Edited by Hiroyuki SAKAKI, M.J.A.)

Abstract: Ultracold atoms in an optical lattice provide a unique approach to study quantum many-body systems, previously only possible by using condensed-matter experimental systems. This new approach, often called quantum simulation, becomes possible because of the high controllability of the system parameters and the inherent cleanness without lattice defects and impurities. In this article, we review recent developments in this rapidly growing field of ultracold atoms in an optical lattice, with special focus on quantum simulations using our newly created quantum many-body system of two-electron atoms of ytterbium. In addition, we also mention other interesting possibilities offered by this novel experimental platform, such as applications to precision measurements for studying fundamental physics and a Rydberg atom quantum computation.

Keywords: quantum simulation, ultracold atom, optical lattice, Hubbard model, SU(N) symmetry, two-electron atom

1. Introduction

Recently, the technique of manipulating individual single quantum systems, such as an atom, ion, and photon, has made dramatic progress. On the other hand, many functional materials, a high- T_c superconductor being a representative example, are strongly correlated quantum many-body systems, studied by various approaches to obtain a deeper understanding of the novel behaviors.¹⁾ Quite often, even a qualitative understanding is difficult to obtain for such quantum many-body systems.

Under these circumstances, a system of ultracold atoms in an optical lattice (see Fig. 1) is regarded as an ideal quantum simulator of quantum many-body systems, because it possesses high degrees of controllability of the system parameters, and it is a quite clean system, free of lattice defects and impurities.^{2)–5)} By developing quantum simulation techniques using this ideal system of ultracold atoms in an optical lattice, it is expected that we can offer

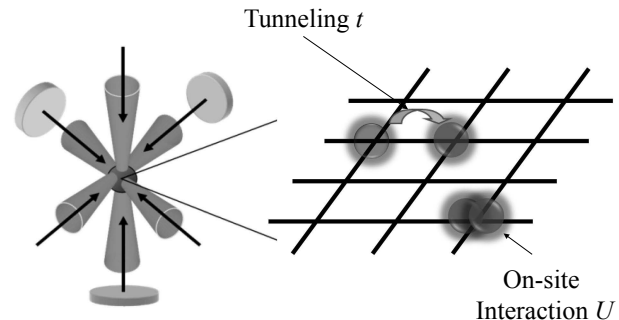


Fig. 1. (Color online) Optical lattice. Laser light whose frequency is far off-resonant with atomic resonances produces a potential for the atoms, and the potential depth is proportional to the light intensity. A periodic potential for atoms is created by the standing waves of laser light. The left panel shows the laser configuration for realizing the 3D optical lattice. When the optical lattice potential depth is so deep that atoms are tightly bound in the lattice sites, such a system can be described with a high degree of precision utilizing a Hubbard model that consists of a tunneling term characterized by the tunneling energy, t , and an on-site interaction term characterized by the on-site energy, U , as shown in the right panel, where the crossed points of the grids represent the optical lattice sites. These important parameters can be precisely tuned by the optical lattice laser intensity and a Feshbach resonance.

*¹ Department of Physics, Graduate School of Science, Kyoto University, Kyoto, Japan.

† Correspondence should be addressed to: Y. Takahashi, Department of Physics, Graduate School of Science, Kyoto University, Oiwakecho, Kitashirakawa, Sakyo-ku, Kyoto 606-8502, Japan (e-mail: takahashi.yoshiro.7v@kyoto-u.ac.jp).

indispensable guidelines for the synthesis of novel functional materials by providing quantitative understandings of strongly correlated many-body systems.

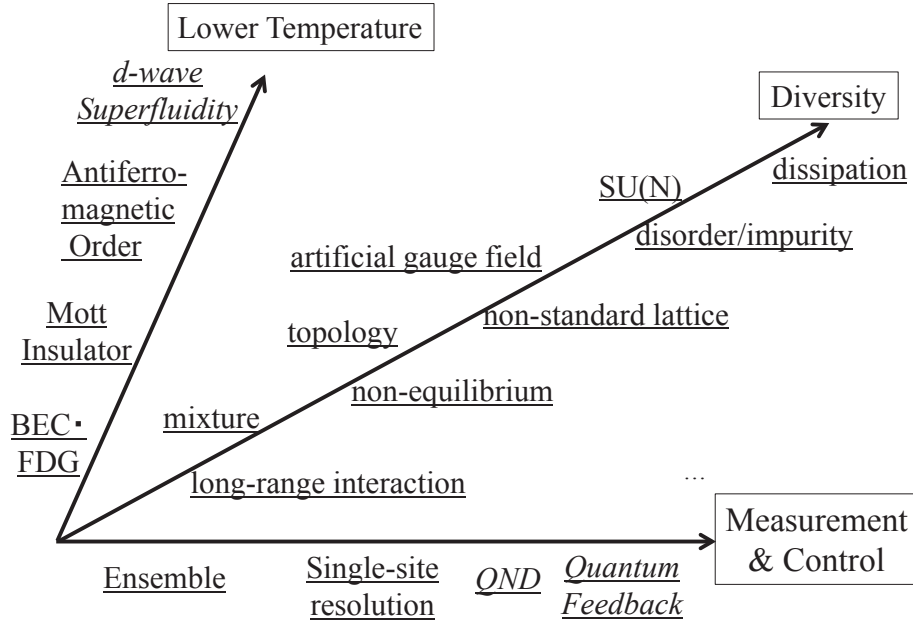


Fig. 2. Achievements and future directions of optical lattice quantum simulation. Lowering the temperature and developing techniques for measurement and control are two important directions of the field. In addition, the diversity of research topics is also an important feature.

The system is also quite useful for the ideal realization of novel topological phases. Thus, quantum simulation research will have potential impacts on our society.

Here, we consider the notion of quantum simulation research using cold atoms in an optical lattice.⁶⁾ Even if one performs some type of experiments using cold atoms in an optical lattice, the work is not always regarded as being a quantum simulation within the framework of quantum information science. For an experiment to be called a quantum simulation, the Hamiltonian of the target system must be clearly defined without any ambiguity, no matter how difficult it is to calculate the static or dynamic properties of the system. From the viewpoint of engineering, quantum simulations are important for computationally hard problems, such as the Fermi-Hubbard model (FHM) and the quench dynamics of the Bose-Hubbard model (BHM), whereas, from a scientific point of view, the target of quantum simulation could include conceptually important phenomena, such as topological quantum phenomena, even if it is computationally not difficult.

Figure 2 summarizes the achievements of optical lattice quantum simulation research as well as its future directions, expressed by italics. Quantum phase transitions for bosons^{7),8)} were successfully observed and quantum magnetism is being actively

studied for fermions by both ensemble measurements^{9)–11)} and a recently developed method involving the site-resolved imaging of individual single atoms, called a quantum gas microscopy (QGM).^{12)–17)} The apparent next step is to lower the temperature of atoms, to realize the expected d-wave superfluidity. Along with the important directions of lowering the temperature and the development of measurement and control techniques, a rich variety of interesting research topics are currently being studied, such as SU(N) spin symmetry, non-standard lattice, topological physics, open quantum dynamics, mixtures, quantum transport, and so on. In Sec. 2–8, we introduce these important topics along with the backgrounds as well as detailed descriptions of our experiments done by using a two-electron atom of ytterbium (Yb). In Sec. 9, in addition to the summary and perspective of the quantum simulation research, we also mention other interesting possibilities offered by this novel experimental platform, such as the applications to precision measurements for the study of fundamental physics¹⁸⁾ and a Rydberg atom quantum computation.¹⁹⁾

Before going into the details of the experiments, here we summarize the implications and unique properties of Yb quantum gas, a new quantum many-body system created and developed in our

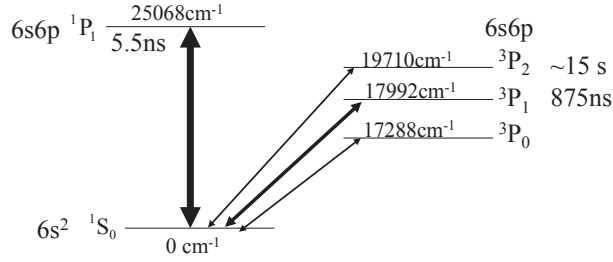


Fig. 3. Relevant low-lying energy levels of an Yb atom. The thickness of the arrows schematically represents the strength of the optical transitions. The 1S_0 - 1P_1 transition gives a strong radiation pressure on the Yb atoms, and is useful for slowing down the high-velocity atomic beam. The 1S_0 - 3P_1 intercombination transition gives a low atomic temperature of 4.4 μ K with Doppler cooling, and is useful for magneto-optical trapping. In addition, there are two ultranarrow optical transitions of 1S_0 - 3P_0 and 1S_0 - 3P_2 , which are useful for two-orbital quantum simulators, precision measurements, and so on.

laboratory over more than two decades.⁵⁾ It is true that alkali atoms are standard atomic species in cold-atom research. However, extending atomic species beyond alkali atoms is important because we can then explore unique possibilities by utilizing atomic species with unique features. In this respect, a rare-earth atom of Yb that possesses the electronic structure of $Xe4f^{14}6s^2$ is quite interesting, because it offers many important possibilities for fundamental research and applications, which are in fact described in this article. One of the unique features of an Yb atom is its energy structure associated with the two-valence electrons. The low-lying energy levels are shown in Fig. 3. There are two ultranarrow optical transitions of 1S_0 - 3P_0 and 1S_0 - 3P_2 . Both transitions have an ultranarrow linewidth of about 10 mHz, and are useful for probing and manipulating the quantum phases as well as constructing novel experimental platforms. Yb has a rich variety of isotopes with five bosons (^{168}Yb , ^{170}Yb , ^{172}Yb , ^{174}Yb , and ^{176}Yb) and two fermions (^{171}Yb and ^{173}Yb). While bosonic isotopes have no spin in the ground state, fermionic isotopes have nuclear spin I ($I = 1/2$ for ^{171}Yb and $I = 5/2$ for ^{173}Yb), which is utilized for SU(N) physics,²⁰⁾ described later. The important parameters of the s-wave scattering lengths which characterize ultracold atomic gases are precisely determined by our two-color photoassociation measurement.²¹⁾ The rich variety of stable isotopes allows us to study not only Bose-Einstein condensate (BEC) and Fermi degenerate gas (FDG), but also quantum degenerate mixtures, such as Bose-Bose, Bose-Fermi and Fermi-Fermi mixtures. Using the laser cooling and evapo-

lative cooling, in fact, we can realize various quantum degenerate gases of Yb atoms,⁵⁾ which are utilized in experiments described in the following sections.

2. Quantum simulation of Fermi-Hubbard model

Strongly correlated many-body systems of electrons play a fundamental role in condensed-matter physics. A central model is the Fermi-Hubbard model (FHM). Quantum simulations of FHM can be performed by using ultracold Fermi gases loaded into an optical lattice.

2.1 Fermi-Hubbard model. FHM is described by the following:

$$H_{\text{SU}(2)\text{FHM}} = -t \sum_{\langle i,j \rangle, \sigma} c_{i,\sigma}^\dagger c_{j,\sigma} + U \sum_i n_{i,\uparrow} n_{i,\downarrow} + \sum_{i,\sigma} \epsilon_i n_{i,\sigma}, \quad [1]$$

where $c_{i,\sigma}$ is a fermionic annihilation operator for site i and spin $\sigma = +1/2(\uparrow)$ or $-1/2(\downarrow)$, $n_{i,\sigma} = c_{i,\sigma}^\dagger c_{i,\sigma}$ is the number operator, and ϵ_i represents the superimposed weak potential. While Eq. [1] contains only the minimum ingredients of the nearest-neighbor hopping, t , and on-site interaction, U , for correlated electrons, it has successfully accounted for diverse phenomena observed in solid-state materials.

For a strong repulsive interaction at a higher temperature, on the one hand, the two-component or SU(2) FHM gives rise to a paramagnetic Mott insulator, which is a dramatic manifestation of quantum many-body effects. At a lower temperature, on the other hand, an antiferromagnetic order emerges below the Néel temperature.^{1),22)} Note that quantum magnetism manifests itself in quantum many-body states of spins coupled by the exchange interaction, and lies at the heart of many fundamental phenomena in condensed-matter physics. In fact, doped 2D SU(2) FHM at low temperatures is a minimum model of high- T_c superconductivity,¹⁾ the complete understanding of which has not been obtained in spite of intensive studies.

2.2. Cold atom SU(2) FHM. The development of experimental implementation of the FHM with ultracold fermionic atoms in optical lattices has provided a new approach for advancing our understanding of strongly correlated fermions.²³⁾ Mott insulating phases have been realized, and studied by various techniques. Recently, an antiferromagnetic order SU(2) FHM¹⁷⁾ has been successfully observed by a QGM technique, where the spatial redistribution of entropy with engineered potential landscapes is utilized for obtaining the ultracold

temperature of $0.25(2)/k_B \times t$. Here, k_B is the Boltzmann constant. Currently, much effort is being devoted for lowering the temperature to realize d-wave superfluidity.

2.3. SU(N) FHM. More than 30 years ago, Ian Affleck and others introduced the SU(N) Hubbard model^{24),25)} as an extension of the conventional SU(2) model, which today attracts much theoretical interest in connection with its exotic quantum phases²⁰⁾ of the SU(N) quantum magnetism, such as chiral spin liquids. The SU(N) FHM is described by the following Hamiltonian:

$$H_{\text{SU(N)FHM}} = -t \sum_{\langle i,j \rangle, \sigma} c_{i,\sigma}^\dagger c_{j,\sigma} + U \sum_{i, \sigma \neq \sigma'} n_{i,\sigma} n_{i,\sigma'} + \sum_{i,\sigma} \epsilon_i n_{i,\sigma}, \quad [2]$$

where now $\sigma = 1, 2, \dots, N$. Note that the hopping matrix element, t , and on-site interaction, U , do not depend on the spin, σ , which assures the SU(N) symmetry. The low-temperature behaviors of the SU(N > 2) model are predicted to be qualitatively different from those of the SU(2) model, mainly due to the enhancement of quantum fluctuation for a large-N system.

2.4. Cold atom SU(N). A rich variety of ultracold atomic systems make it possible to create artificial matter, which is not accessible by traditional condensed-matter systems. The realization of SU(N) FHM is one illustrative example, while SU(N) physics has been discussed in condensed-matter physics, *e.g.*, in the context of heavy-fermion systems for atoms with f-electrons.^{24),25)} For fermionic isotopes of two-electron atoms, such as ytterbium (^{173}Yb) and strontium (^{87}Sr) in the ground $^1\text{S}_0$ and metastable $^3\text{P}_0$ states, the nuclear spin degrees of freedom are decoupled from the electron angular momentum, and thus the inter-atomic interaction does not depend on the spin, σ . This allows us to ideally realize the SU(N = 2I + 1) FHM for nuclear spin I. The positive scattering lengths $a = 10.55 \text{ nm}$ for ^{173}Yb and $a = 5.09 \text{ nm}$ for ^{87}Sr correspond to repulsive interactions ($U > 0$), which is a case of interest in strongly correlated many-body systems.

How can we measure the spin distribution? For alkali-atoms with a large magnetic moment originated from electron spins, a magnetic-field gradient on the order of several Gauss/cm is sufficient for separately imaging each of the spin components by a Stern-Gerlach effect. However, the magnetic moments of nuclei of the SU(N) systems are too weak for this purpose. We have developed an optical Stern-Gerlach effect which utilizes the gradient of a pseudo-

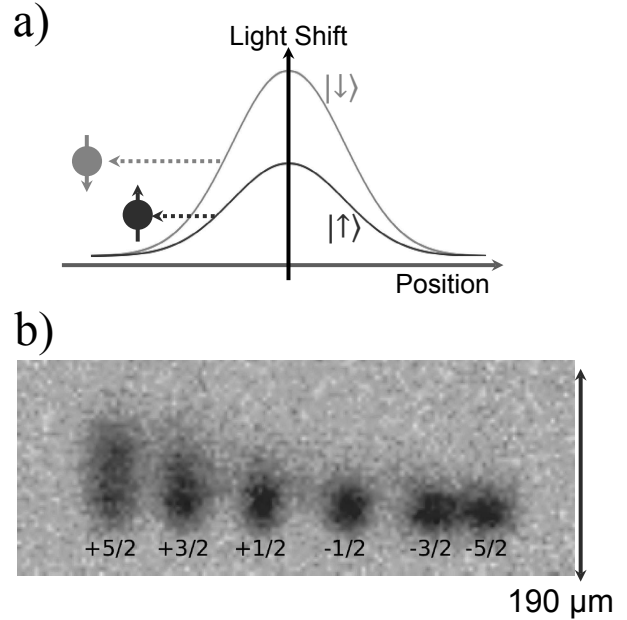


Fig. 4. (Color online) Optical Stern-Gerlach spin measurement. (a) Schematic of the principle of the method. Applying the off-resonant laser light results in the spin-dependent light shifts. When the atoms are located at the shoulder of the beam, then the atoms receive a different momentum kick, resulting in a spin-dependent spatial distribution after some free ballistic flight time. (b) Observed spin distribution with an optical Stern-Gerlach effect for ^{173}Yb . The existence of six spin components of $m_F = -5/2, \dots, +5/2$ is confirmed.

magnetic field created by off-resonant laser light, and is thus also useful for nuclear spin systems.²⁶⁾ Figure 4 indicates the result of optical Stern-Gerlach imaging of the SU(6) spins of ^{173}Yb atoms, which clearly shows the existence of 6 spin components with almost equal weights.

2.5. Cold atom SU(N) experiment: Mott insulator. First, we focus on the realization of a paramagnetic SU(N) Mott insulator.²⁷⁾ There are several signatures for a successful formation of a Mott insulating state. One important feature is the existence of a charge excitation gap. As the U interaction increases, the mobility of atoms is suppressed. Finally, the system enters the incompressible Mott phase when the gap opens. At the same time, a multiple occupation of lattice sites, closely related to the compressibility, $\partial n / \partial \mu$, becomes energetically unfavorable, and is suppressed in the Mott regime. In addition to these features of a Mott insulator, it is also interesting to clarify the difference between the behaviors of Mott insulators with SU(2) and SU(N > 2) symmetries.

Based on the double occupancy measurement, several characteristics of a Mott phase, such as the charge excitation gap and incompressibility, have been clearly observed.²⁷⁾ The result of lattice modulation spectroscopy in which we measure the number of doublons created by the application of the lattice amplitude modulation, clearly indicates the charge excitation gap in a strongly-correlated regime. We also measured the rate of the doublon production by applying lattice amplitude modulation. This is sensitive to the nearest-neighbor correlation, and thus to the temperature of the atoms in the lattice. Comparing the results of an SU(6) system with that of a usual SU(2) system under the same conditions clearly reveals that, due to the large entropy $\ln(N)$ carried by spin, significant cooling occurs for the SU(6) system during adiabatic loading into the lattice; in other words, the Mott phase becomes remarkably stabilized for a large-spin system. This effect is analogous to Pomeranchuk cooling in solid ^3He .²⁸⁾

2.6. Cold atom SU(N) experiment: quantum magnetism. Second, we focus on the spin correlations of the atoms in an optical lattice.¹¹⁾ The detection of spin correlations is important for characterizing quantum many-body states in optical lattices. For the SU(2) Hubbard model, antiferromagnetic correlations were observed in dimerized lattices⁹⁾ that consist of uncoupled two-site systems with enhanced inter-site hopping, and thus large exchange interactions, uniform 3D lattices using Bragg spectroscopy,¹⁰⁾ and 1D- and 2D-lattices using quantum gas microscopy.^{14)–17)} We extended the scheme of the singlet-triplet oscillation (STO) method developed for SU(2) systems and successfully obtained clear signals of antiferromagnetic correlations for dimerized lattice¹¹⁾ as well as homogeneous 1D, 2D, and 3D lattices, and the dimensional crossover regimes in our recent work.²⁹⁾ Figure 5 shows the typical STO signals observed for SU(4) systems in a dimerized lattice, from which we can determine the numbers of singlet-pairs (N_S) and triplet pairs (N_T^0) consisting of different spin components. In a separate measurement, we can determine the total atom number, N_{tot} . We thus deduce the important quantities of the normalized STO amplitude, defined as $(N_S - N_T^0)/N_{tot}$, and the singlet-triplet imbalance, defined as $(N_S - N_T^0)/(N_S + N_T^0)$, which characterize the spin correlation. The precise control of the spin degrees of freedom by an optical pumping technique enables one a straightforward comparison of SU(N = 2)- and SU(N = 4)-

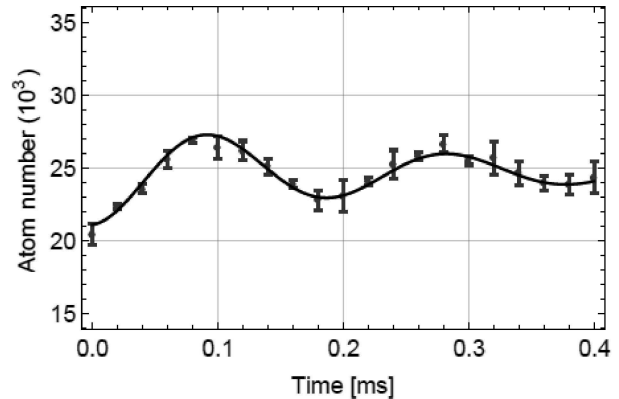


Fig. 5. (Color online) Typical singlet-triplet oscillation (STO) signal observed for the SU(4) system in a dimerized lattice. In a separate measurement, we can determine the total atom number, N_{tot} , and the difference between N_{tot} and the atom number at the beginning of STO corresponds to the singlet-pairs N_S and that between N_{tot} and the atom number after the half cycle of STO triplet pairs, N_T^0 . The clear oscillation indicates an excess of the singlet-pairs over the triplet, corresponding to the antiferromagnetic spin correlation.

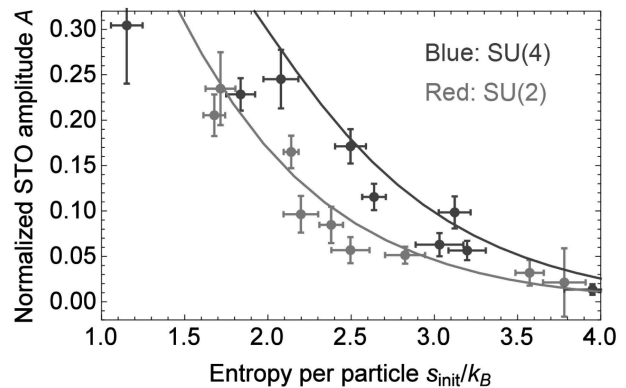


Fig. 6. (Color online) Enhanced Pomeranchuk cooling in quantum magnetism in a dimerized lattice. The normalized STO amplitude is plotted against the initial entropy of the atoms in a harmonic trap before loading to the lattice. The larger STO signal for the SU(4) system, compared with SU(2), indicates realization of the lower temperature of the atoms in the dimerized lattice.

spin systems in the lattice. Figure 6 reveals that the antiferromagnetic spin correlation is enhanced for an SU(4)-spin system compared with SU(2), which indicates that the Pomeranchuk cooling effect is also quite helpful at low temperatures where quantum magnetism manifests itself.

While in the dimerized lattice we enhance the exchange interaction coupling by enhanced tunneling within the dimer, even in homogeneous lattices, where no apparent mechanism of artificially enhanc-

ing the spin correlation, we have clearly observed the nearest-neighbor antiferromagnetic spin correlations of ultracold atoms with SU(6) spin symmetry in optical lattices in our recent work.²⁹⁾ State-of-the-art theoretical calculations based on exact diagonalization and determinantal quantum Monte-Carlo reveal that the experimental data for 1D agrees with theory in which no fitting parameters exist. Remarkably, a comparison with theory implies that the achieved temperature is as low as about 0.1 of the tunneling energy, which is the lowest among experiments ever reported with ultracold fermions. For other dimensions, experimentally achieved correlations are already higher than the regime where theoretical calculations easily converge, while highlighting the experiments as quantum simulations.

3. Quantum simulation with a non-standard lattice

The many-body properties of a quantum system drastically depend on the geometry of an underlying lattice structure. The high flexibility of optical lattice systems enables one to realize several important non-standard lattice structures.³⁰⁾

3.1. Non-standard lattice. Some types of lattices exhibit novel energy-band dispersions, while the kinetic energy of a massive particle generally has a quadratic dependence on its momentum. A honeycomb lattice,³¹⁾ for example, gives rise to a linear dispersion, called a Dirac cone, and has been the target of numerous studies. A more exotic situation is totally vanishing dispersion, called a flat band.^{32),33)} The macroscopic degeneracy in the flat band causes the emergence of localized eigenstates, and has been a key concept in the context of itinerant ferromagnetism for electrons.^{34)–36)} A well-known example having a flat band is a kagome lattice structure,³⁷⁾ which has also been the target of extensive research.

3.2. Lieb lattice. Figure 7(a) shows a lattice structure, called a Lieb lattice, which consists of three sublattices A, B, and C: A-sites form a standard square lattice and the others, B- and C-sites, lie on every line of the square lattice, and thus also called a line-centered square lattice.³⁸⁾ This Lieb lattice also has a flat dispersion in the second band and a Dirac cone on the corner of the Brillouin zone in the tight binding model, as shown in Fig. 7(b).

To derive this band structure, it is convenient to take plane waves on each sublattice $|\mathbf{k}, A\rangle$, $|\mathbf{k}, B\rangle$, and $|\mathbf{k}, C\rangle$ with a momentum \mathbf{k} as a basis set. The existence of only nearest-neighbor tunneling, J , between A and B and that between A and C induces

couplings among these basis states. The resulting tight-binding Hamiltonian, \hat{H}_{TB} , can be written as

$$\hat{H}_{\text{TB}} = \sum_{\mathbf{k}} \begin{pmatrix} \hat{a}_{\mathbf{k},A}^\dagger & \hat{a}_{\mathbf{k},B}^\dagger & \hat{a}_{\mathbf{k},C}^\dagger \end{pmatrix} T \begin{pmatrix} \hat{a}_{\mathbf{k},A} \\ \hat{a}_{\mathbf{k},B} \\ \hat{a}_{\mathbf{k},C} \end{pmatrix}, \quad [3]$$

where T is a 3×3 matrix that couples each sublattice, given by

$$T = \begin{pmatrix} 0 & -2J \cos(k_x d/2) & -2J \cos(k_y d/2) \\ -2J \cos(k_x d/2) & 0 & 0 \\ -2J \cos(k_y d/2) & 0 & 0 \end{pmatrix}. \quad [4]$$

The energy eigenvalues and eigenstates are obtained by diagonalization in a straightforward way, and the energy of the second band is zero with the eigenstate given by

$$|\mathbf{k}, 2\text{nd}\rangle = \cos \theta_{\mathbf{k}} |\mathbf{k}, B\rangle - \sin \theta_{\mathbf{k}} |\mathbf{k}, C\rangle, \quad [5]$$

where $\tan \theta_{\mathbf{k}} = \cos(k_x d/2) / \cos(k_y d/2)$. This corresponds to the flat band shown in Fig. 7(b).

For bosons, interplay between frustrated kinetic energy and inter-atomic interactions is considered to support exotic phases, like supersolids.^{32),33)} For fermions, the celebrated Lieb's theorem predicts the emergence of nonzero magnetization with their Fermi level lying at the flat band.^{34)–36)} Note that the structure of the Lieb lattice is identical to the three-band d - p model, which describes the CuO₂ plane of high- T_c superconductors.³⁹⁾

3.3. Matter wave localization in an optical Lieb lattice. It is obvious that optical-lattice realization of the Lieb lattice for ultracold atoms should provide a unique and powerful quantum simulation of a quantum many-body system for both fermions and bosons. By superimposing three different kinds of optical lattices, we successfully realize the Lieb lattice with high controllability of the lattice parameters.³⁸⁾ In particular, fast control of the lattice potential can imprint a periodic phase on an atomic condensate. This technique provides important means to transfer a Bose condensate prepared in the ground dispersive band of the Lieb lattice into the initially unoccupied flat band. Furthermore, dynamical control of the energy bands allows us to observe occupation numbers of three sublattices in the Lieb lattice with a so-called sublattice mapping technique, which enables us to investigate the stability of the atoms in a flat band.

The highlight is the successful observation of the localized nature of a wave function in the flat band,

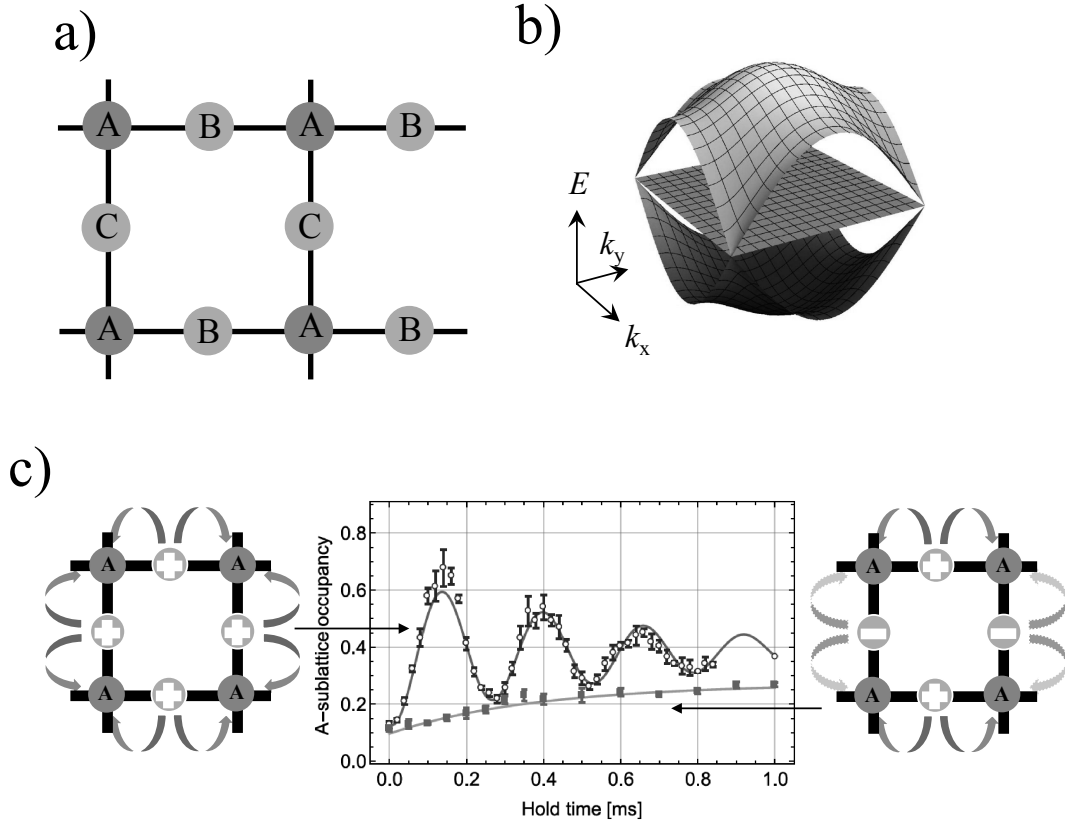


Fig. 7. (Color online) Lieb lattice. (a) Lattice structure. A Lieb lattice is a bi-partite lattice consisting of A-site as well as B- and C-sites. (b) Band structure. The tight-binding energy dispersion shows the existence of flat band and Dirac cones. (c) Matter-wave localization. When the atoms are prepared in the flat band, represented by $(|B\rangle - |C\rangle)/\sqrt{2}$ (right panel), the population of the A-site, which is plotted in the figure in the middle panel as a function of time after the state preparation, is suppressed, even though tunneling between the A-sites and B- and C-sites is allowed (red data in the middle panel), indicating the localization of atoms. In contrast, we have observed the sizable population in the A-site (blue data in the middle panel) when the atoms are prepared in the dispersive band represented by $(|B\rangle + |C\rangle)/\sqrt{2}$ (left panel). Here, the observed oscillation corresponds to the constructive interference of coherent tunnelings between the A- and B-sites and the A- and C-sites.

shown as filled squares in Fig. 7(c). This is caused by destructive interference between the hopping from B- to A-sites and that from C- to A-sites, which is the origin of the unique behaviors of quantum particles in a flat band. In contrast, in a usual dispersive band, shown as open circles in Fig. 7(c), the constructive interference of the tunneling results in delocalization of the atoms.

3.4. Spatial adiabatic passage: transport without transit. In addition, we find a close analogy between the coherent tunnel-coupled three sublattices in the Lieb lattice and the coherent laser-coupled three internal states in an atomic system.⁴⁰⁾ The Hamiltonian of the coherent laser-coupled three-level system is described by the following Hamiltonian:

$$H = \begin{pmatrix} 0 & \Omega & \Omega \\ \Omega & 0 & 0 \\ \Omega & 0 & 0 \end{pmatrix}. \quad [6]$$

Here, Ω is the Rabi-frequency representing the coherent laser coupling between the $|A\rangle$ and $|B\rangle$ states as well as that between $|A\rangle$ and $|C\rangle$. We now consider the Hilbert space spanned by $|A\rangle$, $|B\rangle$, and $|C\rangle$. When one compares Eqs. [4] and [6], the analogy to a Λ -type system is now obvious: momentum-dependent couplings play a role of Rabi couplings in a three-level system.

In quantum optics, a well-known phenomenon unique to the three-level system coherently coupled via two optical fields is the so called Stimulated Raman Adiabatic Passage (STIRAP) process, which

was developed in the 1980's, and has been a robust and efficient way for transferring atomic/molecular internal quantum states in spite of lossy intermediate states.⁴⁰⁾ A key ingredient for the STIRAP is the existence of a dark state, which consists only of the initial and final states with no contribution of the intermediate optically excited states, and thus does not couple with the laser light. As is readily known from Eq. [6], a dark state, $(|B\rangle - |C\rangle)/\sqrt{2}$, arises as one of the eigenstates of the Hamiltonian, Eq. [6].

Thus, the analogy between the Lieb lattice and laser-coupled three-level system suggests the realization of a matter-wave analogue of the STIRAP, meaning that a massive particle moves without any practical possibility of being found at the intermediate area under the situation where the initial and final states are spatially well separated. Such processes, named spatial adiabatic passage (SAP), offer paradoxical *transport without transit*.^{41),42)} Figure 8 shows the experiment of SAP.⁴³⁾ After the counter-intuitive sequence of the dynamical control of tunneling amplitudes, the atoms initially located in B-site move to C-site with the population in the intermediate A-site kept minimally small. This is the first realization of SAP for massive particles. Notice that the flat band consists only of the sublattices B and C with no contribution of the corner A-site. It is the flat band that is responsible for the role of the dark state in the STIRAP. Our work has shed light

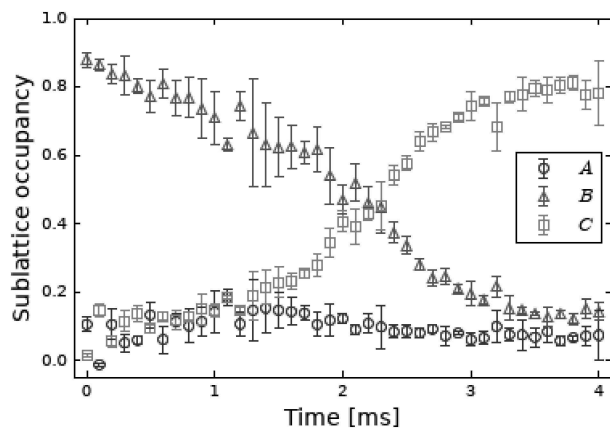


Fig. 8. (Color online) Spatial adiabatic passage. Initially, most of the atoms are prepared only at the B-site (green triangle). The counter-intuitive sequence for transferring the atoms from the B-site to the C-site (red square), consisting of the increase, and later decrease, of the tunneling between the A- and C-sites, followed by the increase and later decrease of the tunneling between the A- and B-sites, results in reasonably efficient transfer with no sizable population in the intermediate A-site (blue circle).

on an analogy between the laser-coupled atomic energy levels and the spatial degrees of freedom of atoms in optical lattices, which provides novel methods of the coherent control in ultracold atomic systems.

4. Quantum simulation of Thouless pump

Topology is an important concept in physics. In condensed matter systems, the best-known example would be the integer quantum Hall effect (IQHE). In a celebrated paper⁴⁴⁾ by Thouless, Kohmoto, Nightingale, and den Nijs (TKNN), they showed that a topological invariant, the sum of the Chern number over the two-dimensional magnetic Brillouin zone of filled bands, gives a quantized value of the Hall conductance. A quantum simulation of topological quantum phenomena is performed by utilizing the high controllability of optical lattice systems.

4.1. Thouless pump. In 1983, Thouless also considered an electron gas in an infinite one-dimensional periodic potential driven by a periodic cycle to discuss the conductive property of the polyacetylene.⁴⁵⁾ He showed that the charge transferred by this system in each “pumping” cycle is quantized, and that the quantization of this charge pumping shares the same topological origin as the IQHE. More specifically, the amount of pumped charge per cycle can be expressed by the Chern number over the (1+1) dimensional Brillouin zone. Therefore, the Thouless pump can, in principle, be a very accurate standard for electric current, just like the Quantum Hall conductance is the standard for electric resistance with extremely high accuracy due to its topological robustness. However, Thouless’s type of the charge pumping device with sufficiently long spatial periodicity has not been realized in electronic systems.

4.2. Cold atom realization of a Thouless pump. Researchers in the field of ultracold atoms have started to realize various topologically-nontrivial systems by exploiting the controllability of ultracold atoms in optical lattices.⁴⁶⁾ In particular, we successfully demonstrated the Thouless charge pump^{47),48)} by constructing a controllable one-dimensional periodic potential consisting of an optical superlattice and loading ultracold fermionic ¹⁷¹Yb atoms instead of electrons. More specifically, we realized the specific lattice model of a Rice-Mele model given in Eq. [7],

$$H_{\text{RM}} = \sum_i (-(J + \delta)a_i^\dagger b_i - (J - \delta)a_i^\dagger b_{i+1} + \text{h.c.} + \Delta(a_i^\dagger a_i - b_i^\dagger b_i)), \quad [7]$$

where a_i and b_i are fermionic annihilation operators in the two sublattices of the i -th unit cell; $J \pm \delta$ is the tunneling amplitude within and between unit cells, respectively, and Δ denotes a staggered on-site energy offset. Thouless pumping in the Rice-Mele model is performed by temporally changing the dimerized hopping amplitude, δ , and the staggered energy, Δ . Therefore, a particular pumping sequence corresponds to a particular trajectory in the δ - Δ parameter space, and the topology of the Thouless pump is determined by whether the trajectory encircles the degeneracy point of $\delta = \Delta = 0$. Figure 9(a) shows a typical pumping sequence and the corresponding lattice potentials at representative times.

As shown in Fig. 9(b), we clearly observed the quantization of Thouless pumping as the quantized shift of the atomic cloud. This is equivalent to a direct measurement of the Chern number of the system. To highlight the topological feature of the pumping, we performed measurements with several topologically-distinct pumping sequences, and compared the amount of pumping. The results are shown in Fig. 9(c). For trajectories which enclose the degeneracy point, the quantized Thouless pump is observed, irrespective of the details of the trajectory, on one hand. For a trajectory that does not enclose the degeneracy point, on the other hand, no pump is observed. These observations illustrate the topological nature of the Thouless pump.

4.3. Disorder induced pump. In addition, we experimentally revealed a surprising effect of quasi-periodic disorder in Thouless quantum pumping in our recent study.⁴⁹⁾ Specifically, we discovered a counter-intuitive phenomenon of disorder-induced pumping in which the presence of disorder induces a non-trivial pump, instead of suppressing, while no pump is observed under a clean condition. This non-trivial phenomenon is a (1+1) dimensional analogue of the seminal topological Anderson insulator,⁵⁰⁾ which has recently attracted so much attention from both theory and experiment. Since the pioneering work by Niu and Thouless in 1984,⁵¹⁾ the problem of topology and disorder has been a crucially important classic problem, but has not been fully understood so far.

Our experimental observations not only demonstrate the realization of a disorder-induced pump, but also quantitatively reveals the degree of robustness and breakdown of the Thouless pump against disorder. The pumped charge keeps its quantized value even at disorder strengths comparable to the

Anderson-localization transition point. The pumped charge drastically decreases when the disorder strength exceeds the threshold value determined by the pump parameters. In addition, our further measurement suggests that the gap closes at the threshold of the disorder strength, indicating that the disorder induces a topological phase transition from topologically non-trivial to trivial phases. Our system offers a unique platform for studying various disorder-related novel effects for a wide range of topological quantum phenomena.

5. Quantum simulation of open quantum system

For a deeper understanding of the physical phenomena in real materials and the development of quantum mechanical devices, it is important to clarify how the dissipation influences the quantum many-body system. The effect of the quantum state by dissipation is often regarded as the observation, crucially important in quantum theory. In addition, recent theories predict the novel role of the dissipation as a tool for preparing and stabilizing some particular quantum states of interest.^{52),53)}

5.1. Dissipation in cold atom experiment.

Ultracold atoms in an optical lattice is an ideal closed quantum many-body system, isolated from the external environment in a vacuum chamber, and is also ideal for studying open quantum systems by artificially introducing dissipation processes in a well-controlled manner. The introduction of a one-body dissipation has been experimentally realized with several methods, such as an electron beam,⁵⁴⁾ and a well-controlled photon scattering process.⁵⁵⁾ Our recent experimental studies of the Parity-Time-symmetric quantum many-body system of bosons have utilized one-body atom loss as dissipation.⁵⁶⁾ A three-body loss process⁵⁷⁾ has been introduced by utilizing a Feshbach resonance.⁵⁸⁾ Since a two-body process plays an important role in quantum phase transitions, investigating the effect of two-body loss process is especially interesting. Along this line of research, the stability of the molecules in a Mott insulating state was investigated so far by using the intrinsic inelastic nature of molecular collisions.^{59),60)}

5.2. Driven, dissipative Hubbard model. We performed a systematic study of the effect of dissipation on a prototypical quantum phase transition in a Bose-Hubbard model, namely the one between the Mott insulator and superfluid phases.⁶¹⁾ We successfully realized a driven-dissipative Bose-Hubbard system in a three-dimensional optical lattice by employing photo-association techniques

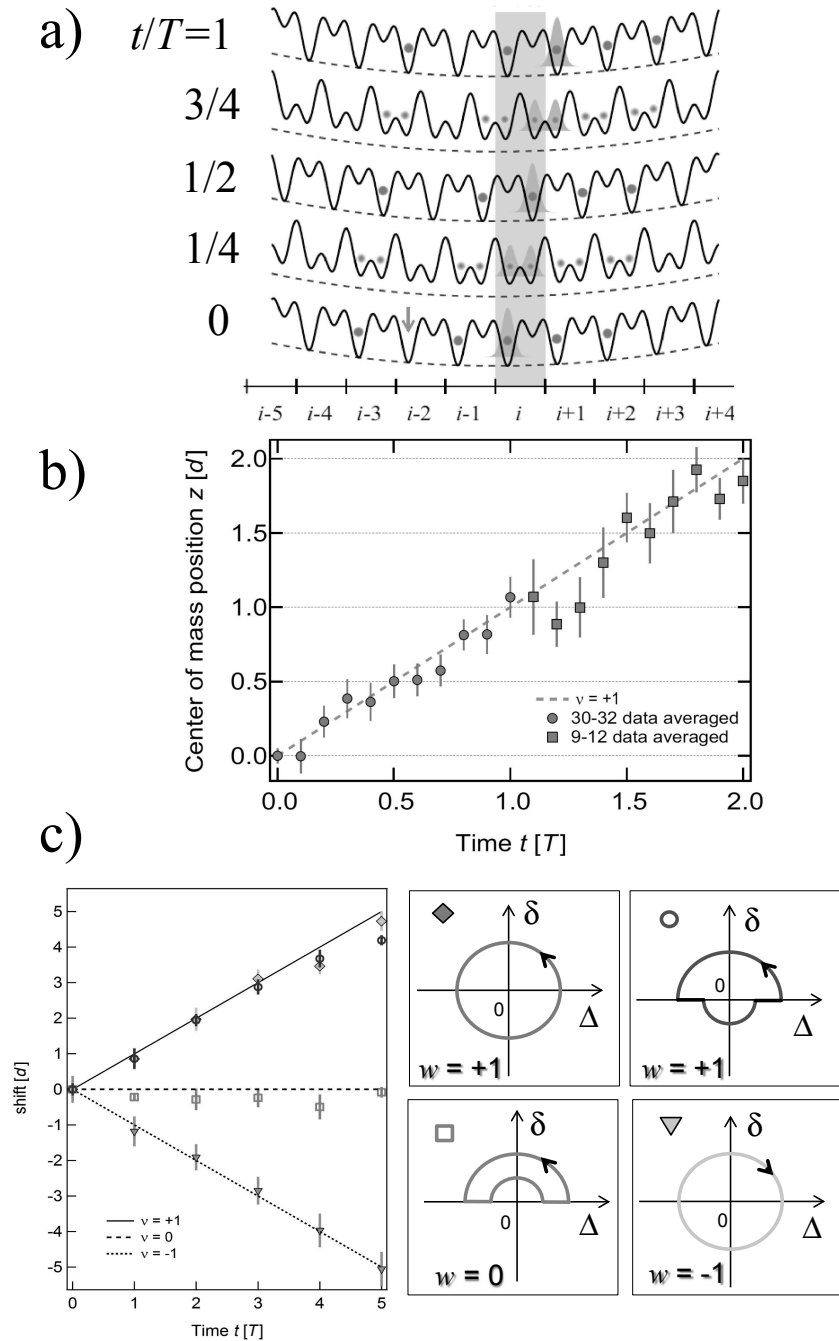


Fig. 9. (Color online) Thouless pump using cold atoms. (a) Typical pumping sequence of Thouless pump. The dimerized lattice potential is periodically modulated with a period of T . The corresponding lattice potential (solid lines) and the atom distribution (red circles) within the lattice are shown. Note that our observable is the shift of the center-of-mass position of the whole atom cloud in a weak harmonic confinement (blue dashed lines), and there are in general holes in the lattice indicated by the arrow. This schematic figure shows the shift of the atoms by exactly one unit cell (light blue area). (b) Quantized Thouless pump. The shift of the center-of-mass position in units of lattice constant d is plotted as a function of the pumping time in units of the period T , or the number of the cycle. The data points are well fitted with a linear line corresponding to the Chern number 1. (c) Topological nature of a Thouless pump. Similar plots, as in (b), are shown for various sequences. The diamonds and circles represent the trajectories encircling the degeneracy point of the origin in the δ - Δ parameter space in a different way, resulting in the same pumping behavior. The inverted triangle represents the trajectory encircling the degeneracy point, but with reverse direction, resulting in the reverse direction of pumping. The square does not encircle the degeneracy point, resulting in no pumping.

to engineer two-body inelastic collisions with a controllable strength. Thus, this system can be described by the following master equation for density operator ρ :

$$\hbar \frac{d}{dt} \rho = -i[H_{\text{BHM}}, \rho] + L_2(\rho), \quad [8]$$

where

$$H_{\text{BHM}} = -t \sum_{\langle i,j \rangle} b_i^\dagger b_j + U \sum_i n_i(n_i - 1)/2 \quad [9]$$

is a single-component Bose-Hubbard Hamiltonian with b_j being a boson annihilation operator. Also,

$$L_2(\rho) = \frac{\hbar\Gamma}{4} \sum_i (-b_i^\dagger b_i^\dagger b_j b_j \rho - \rho b_i^\dagger b_i^\dagger b_j b_j + 2b_j b_j \rho b_i^\dagger b_i^\dagger), \quad [10]$$

where Γ denotes the strength of the two-body loss induced by photoassociation.

Figure 10(a) shows the result of the number of atoms remaining after applying the two-body dissipation, which clearly indicates that a sufficiently strong dissipation inhibits the coherent tunneling motion of the atoms. This is nothing but a manifestation of the quantum Zeno effect.⁶²⁾

Figure 10(b) represents the results on the effect of two-body dissipation on the superfluid-Mott insulator quantum phase transition. In dynamics

subjected to a slow ramp-down of the optical lattice, we have found a novel role of dissipation where strong dissipation favors the Mott insulating state: melting of the Mott insulator is delayed and growth of the phase coherence is suppressed. Notice that the absence of coherence peaks in this case does not mean that the state under dissipation is thermal. This is justified by our experimental confirmation of restoration of the coherence after turning off the dissipation.

It is also interesting to study driven, dissipative FHM in which quantum magnetism within the dimerized lattice is dynamically controlled by utilizing two-body atom loss.^{63),64)}

The present work provides us with a new method for experimental investigations of quantum many-body systems with controllable dissipation and, therefore, stimulates further studies on quantum phase transition phenomena in Liouvillian dynamics.

6. Quantum simulation with atomic mixtures

Since the inter-atomic interaction plays a crucial role in the formation of a Mott insulator state, we can easily imagine that a combined system of two different Mott insulators with strong interspecies interactions will show drastically new features, instead of just the simple sum of the two systems,

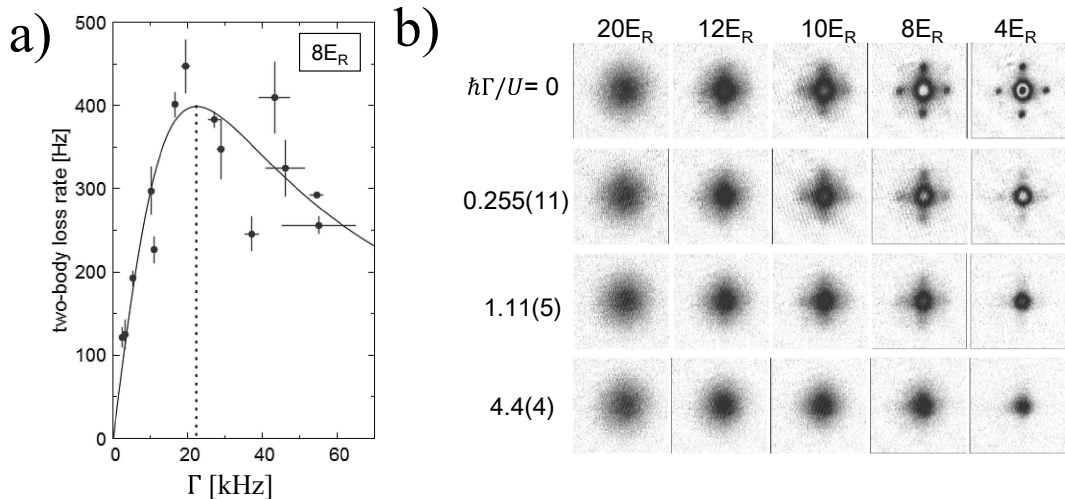


Fig. 10. (Color online) Effect of dissipation on the Bose-Hubbard model. (a) Quantum Zeno effect. The rate of the two-body loss, which results only from tunneling at the lattice height of $8 E_R$, is plotted as a function of the strength of the two-body photoassociation dissipation, Γ . Here, E_R represents the recoil energy, which corresponds to the kinetic energy of the atom with the momentum of a single-photon of the lattice laser light. The counter-intuitive behavior of a decrease in the loss for increased strength of the dissipation is interpreted as being a quantum Zeno effect. (b) Superfluid-Mott insulator transition under dissipation. Time-of-Flight images are shown for various lattice depths after a slow ramping down of the lattice from the Mott insulator. Here, the sharp matter-wave interference peak is a signature of the superfluidity, which is clearly observed at a lattice depth of lower than $8 E_R$, for example, in the case of no dissipation. In contrast, in the presence of the strong dissipation, such a clear interference peak is suppressed even at a shallow depth of $4 E_R$.

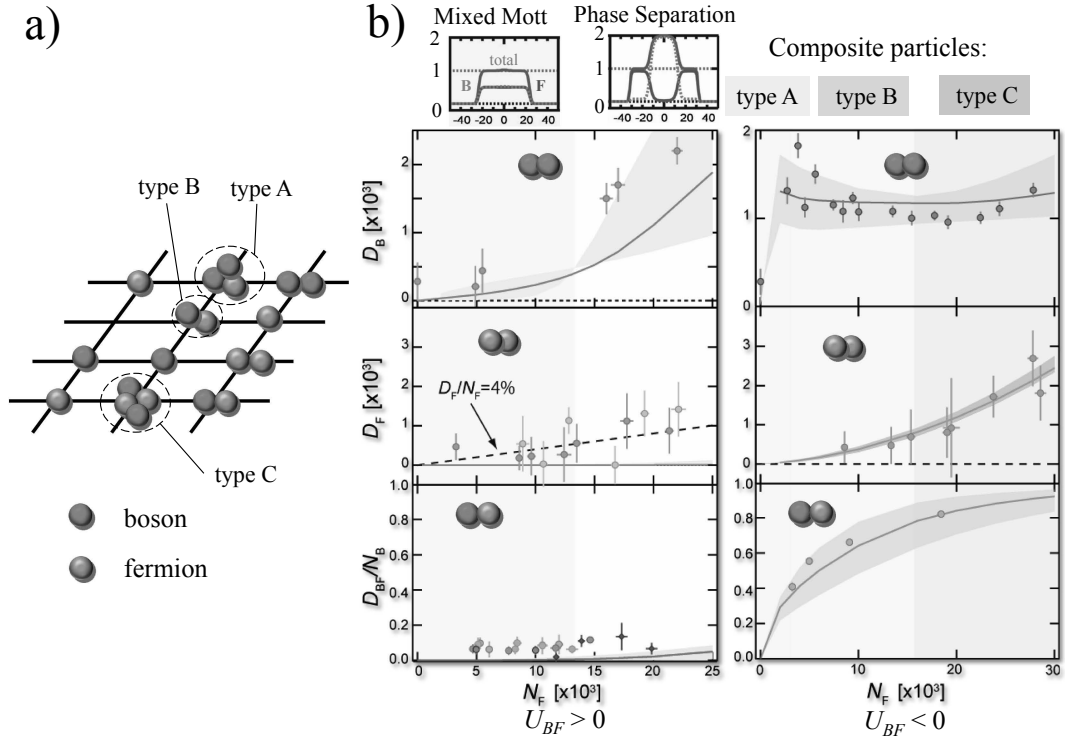


Fig. 11. (Color online) Competition of various phases of a Bose-Fermi dual Mott insulator of repulsively interacting ^{174}Yb - ^{173}Yb and attractively interacting ^{174}Yb - ^{173}Yb . (a) Various pairs in optical lattice sites, which are identified through several photoassociation measurements, such as boson-boson (D_B), fermion-fermion (D_F), and boson-fermion (D_{BF}) pairs. (b) Results of measurements of various pairs indicate that (left panel, ^{174}Yb - ^{173}Yb) bosons and fermions together form a unit-filling Mott insulator at a small number of fermions N_F , whereas the bosonic Mott insulator with double occupancy is phase separated from the unit-filling fermion Mott insulator for larger N_F . On the other hand, (right panel, ^{170}Yb - ^{173}Yb), a Mott insulator is melted, accompanied with the formation of different composite particles of types A, B, and C shown in (a) depending on N_F .

and will enable us to explore the rich phases that are not accessible with a single-component Mott insulator system. Experimental studies on the Bose-Fermi mixture of rubidium (^{87}Rb) and spin polarized potassium (^{40}K) were reported in which the effect of fermions on the bosonic superfluid-Mott insulator transition was studied.^{65)–67)} There are also studies on Bose-Bose and Fermi-Fermi mixtures.

6.1 Dual Mott insulators. By utilizing a rich variety of isotopes of Yb atoms, both for bosons and fermions, we have realized and studied a novel strongly-correlated system of *interacting dual Mott insulators*.⁶⁸⁾ The dual Mott insulators of bosons and fermions can be described by the Hamiltonian (H_{BFHM}) with boson-fermion on-site interactions, U_{BF} , in addition to the bosons (H_{BHM}) and fermions (H_{FHM}),

$$H_{\text{BFHM}} = H_{\text{BHM}} + H_{\text{FHM}} + U_{\text{BF}} \sum_{i,\sigma} n_{B,i} n_{F,i,\sigma}. \quad [11]$$

To characterize dual Mott insulators, we need to measure the double occupancy of bosonic and

fermionic atoms and the pair occupancy of bosons and fermions for varying numbers of atoms, as shown in Fig. 11. Our qualitatively new finding is that the relative filling of atoms and interspecies interaction between atoms drastically modify each Mott insulator, while inducing various interesting quantum phases and their competition. Specifically, we reveal the rich behaviors of atoms, such as melting of a Mott insulator and the generation of various composite particles of boson and fermions in the case of attractive interspecies interactions, and an anti-correlated mixed Mott insulator phase and complete phase-separation in the repulsive case. We have also revealed novel thermodynamic behaviors both for repulsively and attractively interacting cases, and have found evidence of intrinsic adiabatic cooling and heating effects.

6.2. Mixtures with a large mass ratio. Mixtures of large mass ratio are of particular interest, realizing a mixed-dimensional system as an illustrative example. An intriguing possibility is that an

atomic mixture with one species confined in a 2D plane and immersed into a 3D BEC of the other species could result in chiral $p_x + ip_y$ superfluidity by inter-species s-wave interactions.^{69),70)} Here, chiral $p_x + ip_y$ superfluidity has attracted much attention concerning fault-tolerant quantum computation with Majorana modes. In particular, Fermi-Bose mixtures in mixed dimensions support this topological superfluid at relatively higher temperatures for mixtures with a large mass ratio.⁶⁴⁾ In addition, the mixed-dimensional atomic system is interesting for realizing an experimental platform to study an Anderson-Orthogonality catastrophe that results from a Fermi-surface instability induced by a localized impurity.

Experimentally, we have realized quantum degenerate mixtures with a large mass ratio of about 29 with ultracold ^{174}Yb - ^7Li (boson-boson) and ^{173}Yb - ^7Li (fermion-boson) mixtures, as well as ^{174}Yb - ^6Li (boson-fermion) and ^{173}Yb - ^6Li (fermion-fermion).^{71),72)} The quantum degenerate mixtures in a harmonic trap are adiabatically loaded into 3D or 1D optical lattices. While the optical lattice depths are not so different for Yb and Li, the recoil energy, which corresponds to the zero-point energy in the optical lattice site, is species-selective, much smaller for heavy Yb than light Li, realizing novel mixed dimensional systems.^{71),72)}

In addition, our recent efforts have resulted in the successful formation of ^{168}Er - ^6Li and ^{168}Er - ^7Li mixtures. This is another large mass-imbalanced ultracold mixture of atoms and, importantly, the interspecies interaction can be tuned by a Feshbach resonance. The formation and characterization of these ultracold mixtures is a first step towards a possible realizing a topological superfluid in this system as well as novel universal three-body bound states, called Efimov trimers.⁷³⁾

7. Quantum simulation of quantum transport

The Kondo effect⁷⁴⁾ is a quantum many-body phenomenon that arises from an antiferromagnetic spin-exchange interaction between conduction electrons and magnetic impurities. It was originally studied in the context of enhancing the resistivity in magnetic alloys at low temperature, contrary to the monotonic decrease expected for non-interacting fermions, and now it is an ubiquitous problem in condensed-matter physics. The Kondo effect is now one of the important targets of quantum simulation using cold atoms.

7.1. Kondo lattice model. The Kondo lattice

model,⁷⁵⁾ where localized spins are periodically aligned, contains rich physics in the vicinity of the quantum critical point between paramagnetic and magnetically ordered phases, which is described by the following Hamiltonian H_{KLM} :

$$H_{\text{KLM}} = -t_g \sum_{\langle i,j \rangle, \sigma} c_{i,g,\sigma}^\dagger c_{j,g,\sigma} + V_{ex} \sum_{i,\sigma \neq \sigma'} c_{i,g,\sigma}^\dagger c_{i,e,\sigma'}^\dagger c_{i,g,\sigma'} c_{i,e,\sigma}, \quad [12]$$

where t_g is the tunneling amplitude in the conduction band, V_{ex} expresses the spin-exchange energy between the conduction electron and localized impurity, and the symbols g and e represent the conduction and localized bands, respectively.

Competition between the magnetic correlation and localization effects is believed to induce rich quantum phases, represented by a Doniach phase diagram,⁷⁵⁾ in which the paramagnetic phase due to Kondo screening in the strong coupling regime and the Ruderman-Kittel-Kasuya-Yoshida ordered phase in the weak coupling regime are expected.⁷⁶⁾

7.2. Kondo effect with cold atoms. There has been increasing interest on quantum simulations of the Kondo effect by using ultracold atoms in an optical lattice. Several schemes of a cold-atom quantum simulator of the Kondo effect have been proposed for alkali atoms, which require superlattice structures or the population of excited bands, whereas Nishida considers orbital SU(3) Kondo systems by exploiting an confinement-induced resonance.⁷⁷⁾ Recently, two-electron atoms have been intensively studied as an experimental platform with two-orbital degrees of freedom owing to the existence of the metastable state 3P_0 and 3P_2 as well as the ground state 1S_0 . In work by Gorshkov *et al.*,⁷⁸⁾ a two-orbital system using the 1S_0 and 3P_0 states is proposed as a promising candidate for the quantum simulations of the Kondo lattice model.

One of the essential ingredients concerning the mechanism of the Kondo effect is an interorbital antiferromagnetic coupling. The interorbital collisional properties in fermionic isotopes of ^{173}Yb and ^{87}Sr were previously investigated, and the spin-exchange interactions are found to be ferromagnetic. From high-resolution laser spectroscopic measurements of the interorbital spin-exchange interaction for another fermionic isotope of ^{171}Yb , we revealed the inter-orbital scattering lengths to be $a_{eg}^+ = 225(13)a_0$ and $a_{eg}^- = 355(6)a_0$, indicating that the spin-exchange interaction between the two-orbital states is antiferromagnetic, $a_{eg}^+ - a_{eg}^- = -131(19)a_0 < 0$, and large enough to observe the Kondo effect

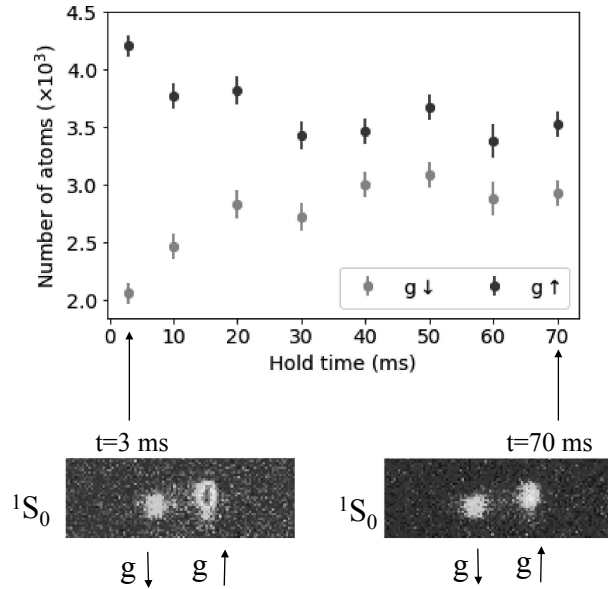


Fig. 12. (Color online) Spin-exchange dynamics between itinerant 1S_0 and localized 3P_0 atoms of ^{171}Yb . The number of spin up (down) in the 1S_0 state, represented as blue (red) circles, is plotted as a function of the hold time at a low magnetic field. The optical Stern-Gerlach images at the hold time of 3 ms and 70 ms are shown.

at currently available atom temperature in an optical lattice.⁷⁹⁾ Here, a_0 represents the Bohr radius.

7.3. Spin-exchange dynamics. In addition, in our recent work,⁸⁰⁾ we have observed the spin-exchange dynamics between ^{171}Yb atoms in the 1S_0 and 3P_0 states by constructing a two-orbital optical lattice. This lattice system realizes a quasi (0+1) D system where the 1S_0 atom behaves as the quasi 1D itinerant free fermions interacting with the 3P_0 atom serving as a localized impurity. As is shown in Fig. 12, we have observed a relaxation of the spin polarization of 1S_0 atoms caused by the interorbital spin-exchange process with the 3P_0 atom. Our work is a first step towards quantum simulations of the Kondo effect using ultracold atoms.

7.4. Atomtronics. There is another type of quantum transport experiment in which one measures the current between terminals, which has been extensively studied so far in solid state materials.^{80),81)} In this type of experiments, the quantized conductance was predicted from the Landauer formula and was demonstrated.

In recent years, the ultracold atom experiments have entered the domain of quantum transport experiments.⁸²⁾ As a result, a new research field of atomtronics has emerged. As a specific example,

researchers created a mesoscopic quantum point contact (QPC) structure for ultracold atoms in real space, and successfully observed the quantization of conductance.⁸³⁾

7.5. Spinor atomtronics. Instead of a spatial degrees of freedom, a novel scheme for quantum transport has been proposed, in which the spin degrees of freedom of ultracold atoms are exploited. This scheme should be called atomtronics with a spin, or *spinor atomtronics*.^{84),85)} Atoms obtain a spin-dependent phase shift via impurity scattering, resulting in quantum transport in Hilbert space spanned by spin. The spin degrees of freedom of the Fermi gas correspond to the terminals and the localized impurity to the QPC.

In recent work,⁸⁶⁾ we successfully demonstrated spin-space quantum transport induced by an atomic QPC using ultracold ^{173}Yb . We elucidate the fundamental properties of the transport dynamics. The unique spin degrees of freedom of ^{173}Yb with $SU(N)$ symmetry have enabled us to successfully realize a three-terminal impurity-induced quantum transport system, which corresponds to the Y-junction. Our work has realized spinor atomtronics, providing unique possibilities in the quantum simulation of quantum transport.

8. Quantum gas microscopy

As is briefly mentioned in the introduction, recently, a QGM technique, which is a method for observing single atoms in an optical lattice with single-site spatial resolution, has been developed for alkali atoms.^{12)–17)} With this powerful technique, we can expect the realization of an ultimate quantum simulator. In fact, the QGM method enables one to observe an antiferromagnetically ordered phase for two-component fermions of alkali atoms loaded into a two-dimensional optical lattice, which is a breakthrough for cold atom FHM research.¹⁷⁾

8.1. QGM of Yb atoms. Extending the QGM technique to atomic species beyond alkali atoms is quite interesting, especially to two-electron atoms, because it will provide intriguing abilities of probing and manipulating each single atom in the quantum simulation work described in this articles, like $SU(N)$ FHM, dual Mott insulators, dissipative Hubbard models, and so on. As a first step, we recently achieved site-resolved imaging of individual ^{174}Yb atoms in a 2D optical lattice.⁸⁷⁾ Figure 13(a) shows the observed image of single Yb atoms in an optical lattice. Figure 13(b) shows the reconstructed lattice sites and the distribution of the individual atoms in

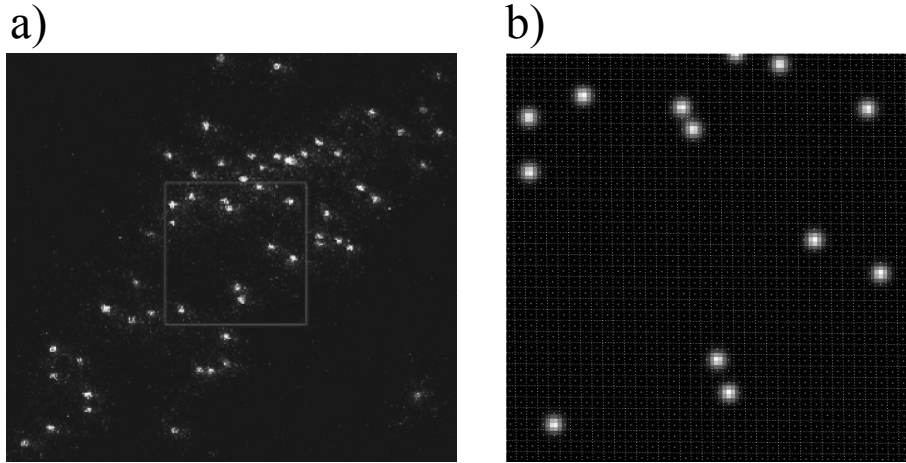


Fig. 13. (Color online) Site-resolved image of individual ^{174}Yb atoms in a two-dimensional optical lattice. During the imaging, the atoms are confined in an extremely deep optical lattice, and irradiated with probe light resonant with the $^1\text{S}_0\text{-}^1\text{P}_1$ transition. To suppress the heating of the atoms during the probing, we also irradiate the atoms with cooling light with the $^1\text{S}_0\text{-}^3\text{P}_1$ transition. (a) Example of the image. (b) Reconstructed atom distribution in the optical lattice for the region designated by the red square in (a). The lattice sites are also superimposed.

the optical lattice within the region indicated by the red square in Fig. 13(a). During probing, we cooled atoms by additionally applying narrow-line laser cooling beams with the $^1\text{S}_0\text{-}^3\text{P}_1$ transition, which is the key of our method. The Yb QGM was also developed in a different method.⁸⁸⁾

In addition, we developed a new kind of method for quantum gas microscopy.⁸⁹⁾ In the conventional quantum gas microscope technique, fluorescent photons due to the irradiated resonant probe light are detected with a high-sensitivity camera. Our new method is based on dispersive interactions between atoms and off-resonant probe light with linear polarization. This dispersive interaction results in a rotation of polarization of the probe light (Faraday rotation), which is detected by a Faraday quantum gas microscope.

8.2. Scheme for quantum non-demolition QGM. One may wonder whether it is possible to perform a quantum non-demolition measurement of single atoms in an optical lattice, which will significantly advance various research on the dynamics of open quantum many-body systems for quantum simulation and quantum information science. Theoretically we clarify the classical non-destructive limit of Faraday quantum gas microscopy using the coherent state of the probe light.⁹⁰⁾ The photon absorption of a probe beam cannot be ignored even in dispersive detection to obtain a signal-to-noise ratio greater than unity because of the shot noise of

the probe beam under a standard measurement condition. Based on this finding, we propose a possible scheme for a quantum non-destructive detection scheme of single atoms in an optical lattice by using a scanning microscope with a squeezed vacuum.⁹⁰⁾

9. Conclusion and prospects

9.1. Conclusions and prospects of quantum simulations. We have reviewed recent progress of quantum simulation research with special focus on the work done by using a quantum many-body systems of two-electron atom Yb. In particular, we describe in detail our recent important work of quantum simulation, such as $\text{SU}(N)$ FHM with enhanced Pomeranchuk cooling effects observed for density distributions and quantum magnetism (Sec. 2), novel flat-band physics in optical Lieb lattice (Sec. 3), the realization of a topological Thouless pump and the novel interplay between topology and disorder (Sec. 4), novel roles of dissipation in quantum phase transitions and quantum magnetism (Sec. 5), quantum simulation of quantum degenerate mixtures (Sec. 6), cold atom realization of quantum transport research (Sec. 7), and the site-resolved imaging of Yb atoms in an optical lattice by a QGM technique (Sec. 8).

So far, all quantum simulation experiments, including those described in this article, were conducted by atomic physics experimentalists using

very complicated, rather large-scaled machines under the well-controlled conditions in their laboratories. An interesting future possibility is remote quantum simulations, in which anyone can run a quantum simulation experiment remotely from home. This novel online system will provide condensed matter theorists with a chance to test the validity of newly developed numerical calculation methods, for example. This remote quantum simulation can also be helpful for a broad range of students to learn important physical concepts, like Bose-Einstein condensation and the superfluid-Mott insulator quantum phase transition as well as the latest technological developments in atomic and condensed matter physics, like a quantum gas microscopy. Efforts along this line have already started in our lab.

9.2. Application to precision measurements.

An experimental platform for quantum simulation using ultracold Yb atoms is also useful for precision measurements to study fundamental physics.¹⁸⁾ We initiated the study involving the laser cooling and trapping of Yb atoms towards tests of time-reversal symmetry by searching for a permanent electric dipole moment. We can expect a long coherence time for individual atoms localized in each site of an optical lattice, free from any inter-atomic interaction. Theoretical calculations show that Yb atoms are sensitive to some CP-violating terms.

Our recent experiment along with the theoretical work has tested Newton gravity at a short range using Yb atoms.^{91),92)} Owing to the lack of a thermal broadening effect for quantum degenerate Yb atoms and the simple molecular potential with neither hyperfine nor singlet-triplet structures, sub-kHz ultra-precise molecular spectroscopy of least-bound molecular levels results in determining the upper-limit of a Yukawa-type correction term.

More recently, precision isotope shift measurements for two-different optical transitions are of intensive interest. Within the framework of the standard model, the obtained isotope shift data sets should satisfy the linearity of a King plot.⁹³⁾ The deviation of the linearity of a King plot indicates the existence of a new particle which mediates the force between an electron and a neutron,⁹⁴⁾ although we should be careful concerning the contribution of higher-order terms of isotope shifts within the standard model to the possible nonlinearity of the King plot. Since Yb has a rich variety of isotopes of 5 bosons and 2 fermions as well as ultra-narrow optical transitions of 1S_0 - 3P_0 and 1S_0 - 3P_0 with a linewidth on the order of mHz, a system of ultracold Yb atoms

and isotope mixtures in an optical lattice, which we have been developing in recent years, offers an ideal experimental platform for this purpose. Efforts along this line have already started in our lab.

A new optical transition of $4f^{14}6s^2: ^1S_0$ - $4f^{13}6s^25d$: ($J = 2$) at 431.2 nm, which has never been observed, is proposed for precision measurements, including testing the time variation of the fine-structure constant.^{95),96)} This transition is also expected to share the advantage of ultra-narrow linewidth.

9.3. Application to quantum computation.

Unique properties of ultracold Yb atoms, especially the rich internal energy levels, have an important application to quantum computing. Recent progress concerning an atom tweezer array using Rydberg states of alkali-atoms is impressive, and a high-fidelity quantum gate has been demonstrated towards realizing quantum computers using neutral atoms.^{19),97)-99)} However, lacking the ability of optical trapping of Rydberg states of alkali-atoms cause serious, though not fatal, problems when one performs quantum gates with reasonable depth. In contrast, owing to the existence of two valence electrons in Yb atoms, one can optically trap Rydberg states, which was recently demonstrated. Various techniques of laser cooling and the manipulation of internal states of Yb atoms, which we have been developed for the purpose of quantum simulation, can be exploited similarly for the development of quantum computing using a Yb atom tweezer array. Efforts along this line have already started in our lab.

Acknowledgements

We greatly thank many collaborators involved both in the experimental and theoretical works, described in this Review. Especially, we thank Y. Takasu, S. Taie, S. Nakajima, N. Takei, J. Kobayashi, R. Yamazaki, S. Kato, H. Ozawa, T. Tomita, R. Yamamoto, K. Shibata, S. Sugawa, K. Ono, F. Schäfer, and H. Konishi for experiment, and I. Danshita, S. Goto, M. Yamashita, K. Inaba, Y. Kuno, S. Uchino, Y. Nishida, L. Wang, K. Hazzard, R. T. Scalettar, E. Ibarra-García-Padilla, and Hao-Tian Wei for theory. This work was partially supported by Grants-in-Aid for Scientific Research of JSPS (Nos. JP17H06138, JP18H05405, and JP18H05228), the Impulsing Paradigm Change through Disruptive Technologies (ImPACT) program, JST CREST (No. JP-MJCR1673), and MEXT Quantum Leap Flagship Program (MEXT Q-LEAP) Grant No. JPMXS0118069021.

References

- 1) Lee, P.A., Nagaosa, N. and Wen, X.-G. (2006) Doping a Mott insulator: Physics of high-temperature superconductivity. *Rev. Mod. Phys.* **78**, 17–85.
- 2) Bloch, I., Dalibard, J. and Zwerger, W. (2008) Many-body physics with ultracold gases. *Rev. Mod. Phys.* **80**, 885–964.
- 3) Esslinger, T. (2010) Fermi-Hubbard physics with atoms in an optical lattice. *Annu. Rev. Condens. Matter Phys.* **1**, 129–152.
- 4) Gross, C. and Bloch, I. (2017) Quantum simulations with ultracold atoms in optical lattices. *Science* **357**, 995–1001.
- 5) Schäfer, F., Fukuhara, T., Sugawa, S., Takasu, Y. and Takahashi, Y. (2020) Tools for quantum simulation with ultracold atoms in optical lattices. *Nat. Rev. Phys.* **2**, 411–425.
- 6) Qiu, X., Zou, J., Qi, X. and Li, X. (2020) Precise programmable quantum simulations with optical lattices. *npj Quantum Inf.* **87**, 1–8.
- 7) Greiner, M., Mandel, O., Esslinger, T., Hansch, T.W. and Bloch, I. (2002) Quantum phase transition from a superfluid to a Mott insulator in a gas of ultracold atoms. *Nature* **415**, 39–44.
- 8) Jaksch, D., Bruder, C., Cirac, J.I., Gardiner, C.W. and Zoller, P. (1998) Cold bosonic atoms in optical lattices. *Phys. Rev. Lett.* **81**, 3108–3111.
- 9) Greif, D., Uehlinger, T., Jotzu, G., Tarruell, L. and Esslinger, T. (2013) Short-range quantum magnetism of ultracold fermions in an optical lattice. *Science* **340**, 1307–1310.
- 10) Hart, R.A., Duarte, P.M., Yang, T.-L., Liu, X., Paiva, T., Khatami, E. *et al.* (2015) Observation of antiferromagnetic correlations in the Hubbard model with ultracold atoms. *Nature* **519**, 211.
- 11) Ozawa, H., Taie, S., Takasu, Y. and Takahashi, Y. (2018) Antiferromagnetic spin correlation of SU(N) fermi gas in an optical superlattice. *Phys. Rev. Lett.* **121**, 225303.
- 12) Bakr, W.S., Gillen, J.I., Peng, A., Fölling, S. and Greiner, M. (2009) A quantum gas microscope for detecting single atoms in a Hubbard-regime optical lattice. *Nature* **462**, 74–77.
- 13) Sherson, J.F., Weitenberg, C., Endres, M., Cheneau, M., Bloch, I. and Kuhr, S. (2010) Single-atom-resolved fluorescence imaging of an atomic Mott insulator. *Nature* **467**, 68–72.
- 14) Boll, M., Hilker, T.A., Salomon, G., Omran, A., Nespolo, J., Pollet, L. *et al.* (2016) Spin- and density-resolved microscopy of antiferromagnetic correlations in Fermi-Hubbard chains. *Science* **353**, 1257–1260.
- 15) Parsons, M.F., Mazurenko, A., Chiu, C.S., Ji, G., Greif, D. and Greiner, M. (2016) Site-resolved measurement of the spin-correlation function in the Fermi-Hubbard model. *Science* **353**, 1253–1256.
- 16) Cheuk, L.W., Nichols, M.A., Lawrence, K.R., Okan, M., Zhang, H., Khatami, E. *et al.* (2016) Observation of spatial charge and spin correlations in the 2D Fermi-Hubbard model. *Science* **353**, 1260–1264.
- 17) Mazurenko, A., Chiu, C.S., Ji, G., Parsons, M.F., Kanász-Nagy, M., Schmidt, R. *et al.* (2017) A cold-atom Fermi-Hubbard antiferromagnet. *Nature* **545**, 462–466.
- 18) Safronova, M.S., Budker, D., DeMille, D., Kimball, D.F.J., Derevianko, A. and Clark, C.W. (2018) Search for new physics with atoms and molecules. *Rev. Mod. Phys.* **90**, 025008.
- 19) Saffman, M. (2016) Quantum computing with atomic qubits and Rydberg interactions: progress and challenges. *J. Phys. B: At. Mol. Opt. Phys.* **49**, 202001.
- 20) Cazalilla, M.A. and Rey, A.M. (2014) Ultracold Fermi gases with emergent SU(N) symmetry. *Rep. Prog. Phys.* **77**, 124401.
- 21) Kitagawa, M., Enomoto, K., Kasa, K., Takahashi, Y., Ciurylo, R., Naidon, P. *et al.* (2008) Two-color photoassociation spectroscopy of ytterbium atoms and the precise determinations of s-wave scattering lengths. *Phys. Rev. A* **77**, 012719.
- 22) Moriya, T. and Ueda, K. (2003) Antiferromagnetic spin fluctuation and superconductivity. *Rep. Prog. Phys.* **66**, 1299–1341.
- 23) Auerbach, A. (2012) *Interacting Electrons and Quantum Magnetism*. Graduate Texts in Contemporary Physics, Springer, New York.
- 24) Affleck, I. (1985) Large- n limit of SU(n) quantum “spin” chains. *Phys. Rev. Lett.* **54**, 966.
- 25) Coleman, P. (2015) Heavy fermions and the Kondo lattice: a 21st century perspective. *In Many-Body Physics: From Kondo to Hubbard* (eds. Pavarini, E., Koch, E. and Coleman, P.). Forschungszentrum, Jülich, Chapter 1.
- 26) Taie, S., Takasu, Y., Sugawa, S., Yamazaki, R., Tsujimoto, T., Murakami, R. *et al.* (2010) Realization of a SU(2)×SU(6) system of fermions in a cold atomic gas. *Phys. Rev. Lett.* **105**, 190401.
- 27) Taie, S., Yamazaki, R., Sugawa, S. and Takahashi, Y. (2012) An SU(6) Mott insulator of an atomic Fermi gas realized by large-spin Pomeranchuk cooling. *Nat. Phys.* **8**, 825–830.
- 28) Richardson, R.C. (1997) The Pomeranchuk effect. *Rev. Mod. Phys.* **69**, 683–690.
- 29) Taie, S., Ibarra-García-Padilla, E., Nishizawa, N., Takasu, Y., Kuno, Y., Wei, H.-T. *et al.* (2020) Observation of antiferromagnetic correlations in an ultracold SU(N) Hubbard model. arXiv2010.07730.
- 30) Windpassinger, P. and Sengstock, K. (2013) Engineering novel optical lattices. *Rep. Prog. Phys.* **76**, 086401.
- 31) Tarruell, L., Greif, D., Uehlinger, T., Jotzu, G. and Esslinger, T. (2012) Creating, moving and merging Dirac points with a Fermi gas in a tunable honeycomb lattice. *Nature* **483**, 302–305.
- 32) Huber, S.D. and Altman, E. (2010) Bose condensation in flat bands. *Phys. Rev. B* **82**, 184502.
- 33) Takayoshi, S., Katsura, H., Watanabe, N. and Aoki, H. (2013) Phase diagram and pair Tomonaga-Luttinger liquid in a Bose-Hubbard model with flat bands. *Phys. Rev. A* **88**, 063613.

- 34) Lieb, E.H. (1989) Two theorems on the Hubbard model. *Phys. Rev. Lett.* **62**, 1201–1204.
- 35) Mielke, A. (1991) Ferromagnetism in the Hubbard model on line graphs and further considerations. *J. Phys. A: Math. Gen.* **24**, 3311–3321.
- 36) Tasaki, H. (1992) Ferromagnetism in the Hubbard models with degenerate single-electron ground states. *Phys. Rev. Lett.* **69**, 1608–1611.
- 37) Jo, G.-B., Guzman, J., Thomas, C.K., Hosur, P., Vishwanath, A. and Stamper-Kurn, D.M. (2012) Ultracold atoms in a tunable optical kagome lattice. *Phys. Rev. Lett.* **108**, 045305.
- 38) Taie, S., Ozawa, H., Ichinose, T., Nishio, T., Nakajima, S. and Takahashi, Y. (2015) Coherent driving and freezing of bosonic matter wave in an optical Lieb lattice. *Sci. Adv.* **1**, e1500854.
- 39) Igloukov, V.I., Hébert, F., Grémaud, B., Batrouni, G.G. and Scalettar, R.T. (2014) Superconducting transitions in flat-band systems. *Phys. Rev. B* **90**, 094506.
- 40) Bergmann, K., Theuer, H. and Shore, B.W. (1998) Coherent population transfer among quantum states of atoms and molecules. *Rev. Mod. Phys.* **70**, 1003–1025.
- 41) Rab, M., Cole, J.H., Parker, N.G., Greentree, A.D., Hollenberg, L.C.L. and Martin, A.M. (2008) Spatial coherent transport of interacting dilute Bose gases. *Phys. Rev. A* **77**, 061602.
- 42) Benseny, A., Bagudà, J., Oriols, X. and Mompert, J. (2012) Need for relativistic corrections in the analysis of spatial adiabatic passage of matter waves. *Phys. Rev. A* **85**, 053619.
- 43) Taie, S., Ichinose, T., Ozawa, H. and Takahashi, Y. (2020) Spatial adiabatic passage of massive quantum particles in an optical Lieb lattice. *Nat. Commun.* **11**, 257.
- 44) Thouless, D.J., Kohmoto, M., Nightingale, M.P. and den Nijs, M. (1982) Quantized Hall conductance in a two-dimensional periodic potential. *Phys. Rev. Lett.* **49**, 405–408.
- 45) Thouless, D.J. (1983) Quantization of particle transport. *Phys. Rev. B* **27**, 6083–6087.
- 46) Goldman, N., Budich, J.C. and Zoller, P. (2016) Topological quantum matter with ultracold gases in optical lattices. *Nat. Phys.* **12**, 639–645.
- 47) Nakajima, S., Tomita, T., Taie, S., Ichinose, T., Ozawa, T., Wang, L. *et al.* (2016) Topological Thouless pumping of ultracold fermions. *Nat. Phys.* **12**, 296–300.
- 48) Lohse, M., Schweizer, C., Zilberberg, O., Aidelsburger, M. and Bloch, I. (2015) A Thouless quantum pump with ultracold bosonic atoms in an optical superlattice. *Nat. Phys.* **12**, 350–354.
- 49) Nakajima, S., Takei, N., Sakuma, K., Kuno, Y., Marra, P. and Takahashi, Y. (2021) Competition and interplay between topology and quasi-periodic disorder in Thouless pumping of ultracold atoms. *Nat. Phys.* **17**, 844–849.
- 50) Li, J., Chu, R.-L., Jain, J.K. and Shen, S.-Q. (2009) Topological Anderson insulator. *Phys. Rev. Lett.* **102**, 136806.
- 51) Niu, Q. and Thouless, D.J. (1984) Quantised adiabatic charge transport in the presence of substrate disorder and many-body interaction. *J. Phys. A: Math. Gen.* **17**, 2453–2462.
- 52) Daley, A.J. (2014) Quantum trajectories and open many-body quantum systems. *Adv. Phys.* **63**, 77–149.
- 53) Müller, M., Diehl, S., Pupillo, G. and Zoller, P. (2012) Engineered open systems and quantum simulations with atoms and ions. *Adv. At. Mol. Opt. Phys.* **61**, 1–80.
- 54) Labouvie, R., Santra, B., Heun, S., Wimberger, S. and Ott, H. (2015) Negative differential conductivity in an interacting quantum gas. *Phys. Rev. Lett.* **115**, 050601.
- 55) Patil, Y.S., Chakram, S. and Vengalattore, M. (2015) Measurement-induced localization of an ultracold lattice gas. *Phys. Rev. Lett.* **115**, 140402.
- 56) Takasu, Y., Yagami, T., Ashida, Y., Hamazaki, R., Kuno, Y. and Takahashi, Y. (2020) PT-symmetric non-Hermitian quantum many-body system using ultracold atoms in an optical lattice with controlled dissipation. *Prog. Theor. Exp. Phys.* **2020**, 12A110.
- 57) Mark, M.J., Haller, E., Lauber, K., Danzl, J.G., Janisch, A., Büchler, H.P. *et al.* (2012) Preparation and spectroscopy of a metastable Mott-insulator state with attractive interactions. *Phys. Rev. Lett.* **108**, 215302.
- 58) Chin, C., Grimm, R., Julienne, P. and Tiesinga, E. (2010) Feshbach resonances in ultracold gases. *Rev. Mod. Phys.* **82**, 1225–1286.
- 59) Syassen, N., Bauer, D.M., Lettner, M., Volz, T., Dietze, D., García-Ripoll, J.J. *et al.* (2008) Strong dissipation inhibits losses and induces correlations in cold molecular gases. *Science* **320**, 1329–1331.
- 60) Yan, B., Moses, S.A., Gadway, B., Covey, J.P., Hazzard, K.R.A., Rey, A.M. *et al.* (2013) Observation of dipolar spin-exchange interactions with lattice-confined polar molecules. *Nature* **501**, 521–525.
- 61) Tomita, T., Nakajima, S., Danshita, I., Takasu, Y. and Takahashi, Y. (2017) Observation of the Mott insulator to superfluid crossover of a driven-dissipative Bose-Hubbard system. *Sci. Adv.* **3**, e1701513.
- 62) Itano, W.M., Heinzen, D.J., Bollinger, J.J. and Wineland, D.J. (1990) Quantum Zeno effect. *Phys. Rev. A* **41**, 2295–2300.
- 63) Sponselee, K., Freystatzky, L., Abeln, B., Diem, M., Hundt, B., Kochanek, A. *et al.* (2018) Dynamics of ultracold quantum gases in the dissipative Fermi-Hubbard model. *Quantum Sci. Technol.* **4**, 014002.
- 64) Nakagawa, M., Tsuji, N., Kawakami, N. and Ueda, M. (2020) Dynamical sign reversal of magnetic correlations in dissipative Hubbard models. *Phys. Rev. Lett.* **124**, 147203.
- 65) Günter, K., Stöferle, T., Moritz, H., Köhl, M. and Esslinger, T. (2006) Bose-Fermi mixtures in a three-dimensional optical lattice. *Phys. Rev. Lett.* **96**, 180402.
- 66) Ospelkaus, S., Ospelkaus, C., Wille, O., Succo, M., Ernst, P., Sengstock, K. *et al.* (2006) Localization

- of bosonic atoms by fermionic impurities in a three-dimensional optical lattice. *Phys. Rev. Lett.* **96**, 180403.
- 67) Best, T., Will, S., Schneider, U., Hackermüller, L., van Oosten, D., Bloch, I. *et al.* (2009) Role of interactions in 87Rb-40K Bose-Fermi mixtures in a 3d optical lattice. *Phys. Rev. Lett.* **102**, 030408.
- 68) Sugawa, S., Inaba, K., Taie, S., Yamazaki, R., Yamashita, M. and Takahashi, Y. (2011) Interaction and filling-induced quantum phases of dual Mott insulators of bosons and fermions. *Nat. Phys.* **7**, 642–648.
- 69) Wu, Z. and Bruun, G.M. (2016) Topological superfluid in a Fermi-Bose mixture with a high critical temperature. *Phys. Rev. Lett.* **117**, 245302.
- 70) Caracanhas, M.A., Schreck, F. and Smith, C.M. (2017) Fermi-Bose mixture in mixed dimensions. *New J. Phys.* **19**, 115011.
- 71) Schäfer, Mizukami, N., Yu, P., Koibuchi, S., Bouscal, A. and Takahashi, Y. (2018) Experimental realization of ultracold Yb-7Li mixtures in mixed dimensions. *Phys. Rev. A* **98**, 051602(R).
- 72) Konishi, H., Schäfer, F., Ueda, S. and Takahashi, Y. (2016) Collisional stability of localized Yb(3P₂) atoms immersed in a Fermi sea of Li. *New J. Phys.* **18**, 103009.
- 73) Naidon, P. and Endo, S. (2017) Efimov physics: a review. *Rep. Prog. Phys.* **80**, 056001.
- 74) Kondo, J. (1964) Resistance minimum in dilute magnetic alloys. *Prog. Theor. Phys.* **32**, 37–49.
- 75) Doniach, S. (1977) The Kondo lattice and weak antiferromagnetism. *Physica B+C* **91**, 231.
- 76) Ruderman, M.A. and Kittel, C. (1954) Indirect exchange coupling of nuclear magnetic moments by conduction electrons. *Phys. Rev.* **96**, 99–102.
- 77) Nishida, Y. (2013) SU(3) orbital Kondo effect with ultracold atoms. *Phys. Rev. Lett.* **111**, 135301.
- 78) Gorshkov, A.V., Hermele, M., Gurarie, V., Xu, C., Julienne, P.S., Ye, J. *et al.* (2010) Two-orbital SU(N) magnetism with ultracold alkaline-earth atoms. *Nat. Phys.* **6**, 289–295.
- 79) Ono, K., Kobayashi, J., Amano, Y., Sato, K. and Takahashi, Y. (2019) Antiferromagnetic interorbital spin-exchange interaction of ¹⁷¹Yb. *Phys. Rev. A* **99**, 032707.
- 80) Ono, K., Amano, Y., Higomoto, T., Saito, Y. and Takahashi, Y. (2021) Observation of spin-exchange dynamics between itinerant and localized ¹⁷¹Yb atoms. *Phys. Rev. A* **103**, L041303.
- 81) Imry, Y. (2002) *Introduction to Mesoscopic Physics*. Oxford University Press, Oxford.
- 82) Krinner, S., Esslinger, T. and Brantut, J.-P. (2017) Two-terminal transport measurements with cold atoms. *J. Phys. Condens. Matter* **29**, 343003.
- 83) Krinner, S., Stadler, D., Husmann, D., Brantut, J.-P. and Esslinger, T. (2015) Observation of quantized conductance in neutral matter. *Nature* **517**, 64–67.
- 84) You, J.-S., Schmidt, R., Ivanov, D.A., Knap, M. and Demler, E. (2019) Atomtronics with a spin: Statistics of spin transport and nonequilibrium orthogonality catastrophe in cold quantum gases. *Phys. Rev. B* **99**, 214505.
- 85) Nakada, S., Uchino, S. and Nishida, Y. (2020) Simulating quantum transport with ultracold atoms and interaction effects. *Phys. Rev. A* **102**, 031302.
- 86) Ono, K., Higomoto, T., Saito, Y., Uchino, Y., Nishida, Y. and Takahashi, Y. (2021) Observation of spin-space quantum transport induced by an atomic quantum point contact. *Nat. Commun.* **12**, 6724.
- 87) Yamamoto, R., Kobayashi, J., Kuno, T., Kato, K. and Takahashi, Y. (2016) An ytterbium quantum gas microscope with narrow-line laser cooling. *New J. Phys.* **18**, 023016.
- 88) Miranda, M., Inoue, R., Okuyama, Y., Nakamoto, A. and Kozuma, M. (2015) Site-resolved imaging of ytterbium atoms in a two-dimensional optical lattice. *Phys. Rev. A* **91**, 063414.
- 89) Yamamoto, R., Kobayashi, J., Kato, K., Kuno, T., Sakura, Y. and Takahashi, Y. (2017) Site-resolved imaging of single atoms with a Faraday quantum gas microscope. *Phys. Rev. A* **96**, 033610.
- 90) Okuno, D., Amano, Y., Enomoto, K., Takei, N. and Takahashi, Y. (2020) Schemes for nondestructive quantum gas microscopy of single atoms in an optical lattice. *New J. Phys.* **22**, 013041.
- 91) Borkowski, M., Buchachenko, A.A., Ciuryło, R., Julienne, P.S., Yamada, H., Kikuchi, Y. *et al.* (2019) Weakly bound molecules as sensors of new gravitylike forces. *Sci. Rep.* **9**, 14807.
- 92) Borkowski, M., Buchachenko, A.A., Ciuryło, R., Julienne, P.S., Yamada, H., Kikuchi, Y. *et al.* (2017) Beyond-Born-Oppenheimer effects in sub-kHz-precision photoassociation spectroscopy of ytterbium atoms. *Phys. Rev. A* **96**, 063405.
- 93) King, W.H. (1963) Comments on the article “Peculiarities of the Isotope Shift in the Samarium Spectrum”. *J. Opt. Soc. Am.* **53**, 638–639.
- 94) Delaunay, C., Ozeri, R., Perez, G. and Soreq, Y. (2017) Probing atomic Higgs-like forces at the precision frontier. *Phys. Rev. D* **96**, 093001.
- 95) Saffronova, M.S., Porsev, S.G., Sanner, C. and Ye, J. (2018) Two clock transitions in neutral Yb for the highest sensitivity to variations of the fine-structure constant. *Phys. Rev. Lett.* **120**, 173001.
- 96) Dzuba, V.A., Flambaum, V.V. and Schiller, S. (2018) Testing physics beyond the standard model through additional clock transitions in neutral ytterbium. *Phys. Rev. A* **98**, 022501.
- 97) Saffman, M., Walker, T.G. and Mølmer, K. (2010) Quantum information with Rydberg atoms. *Rev. Mod. Phys.* **82**, 2313–2363.
- 98) Barredo, D., de Léséleuc, S., Lienhard, V., Lahaye, T. and Browaeys, A. (2016) An atom-by-atom assembler of defect-free arbitrary two-dimensional atomic arrays. *Science* **354**, 1021–1023.
- 99) Endres, M., Bernien, H., Keesling, A., Levine, H., Anschuetz, E.R., Krajenbrink, A. *et al.* (2016) Atom-by-atom assembly of defect-free one-dimensional cold atom arrays. *Science* **354**, 1024–1027.

Profile

Yoshiro Takahashi was born in Gunma Prefecture in 1963. He graduated from Kyoto University in 1986. He received his PhD degree from Kyoto University in 1992. Since 2007 he has been working as Professor of Physics in Graduate School of Science of Kyoto University. His main research topic is ultracold atomic physics, especially quantum simulation research where quantum degenerate atomic gases are loaded into an optical lattice to study novel quantum many-body properties. His recent work also includes precision measurements for fundamental physics. He was awarded Medal with Purple Ribbon (2020) for “study of atomic physics” from the Emperor of Japan, Nishina Memorial Prize (2013) for “Creation of ultracold quantum system of ytterbium” from Nishina Foundation, Hiroshi Takuma Memorial Prize (2012) for “Simulation of quantum many-body system using ultracold atoms trapped in an optical lattice” from Matsuo Foundation, American Physical Society Fellowship (2011) for “For the creation of first two-electron Bose-Einstein condensate and significant contributions to the physics of ultracold degenerate Bose-Fermi mixtures” from American Physical Society, Ryogo Kubo Memorial Prize (2008) for “Realization of an ultra-cold quantum gas of ytterbium atoms” from Inoue Foundation for Science, and Distinguished Research Prize in Optical and Quantum Electronics (2006) for “BEC of ytterbium atoms” with T. Yabuzaki from Japanese Society of Applied Physics.

